Acta Cryst E CRYSTALLOGRAPHIC COMMUNICATIONS

ISSN 2056-9890

Bis(μ_2-*N*-methyl-*N*-phenyldithiocarbamato)-κ^3S,S':S;κ^3S:S,S'-bis[(*N*-methyl-*N*-phenyldithiocarbamato-κ^2S,S')cadmium]: crystal structure and Hirshfeld surface analysis

Siti Aisyah Nabilah Suwardi,[a] See Mun Lee,[b]* Kong Mun Lo,[b] Mukesh M. Jotani[c] and Edward R. T. Tiekink[b]*

[a]Department of Chemistry, University of Malaya, 50603 Kuala Lumpur, Malaysia, [b]Research Centre for Crystalline Materials, School of Science and Technology, Sunway University, 47500 Bandar Sunway, Selangor Darul Ehsan, Malaysia, and [c]Department of Physics, Bhavan's Sheth R. A. College of Science, Ahmedabad, Gujarat 380 001, India. *Correspondence e-mail: annielee@sunway.edu.my, edwardt@sunway.edu.my

Received 15 February 2017
Accepted 16 February 2017

Edited by W. T. A. Harrison, University of Aberdeen, Scotland

Keywords: crystal structure; cadmium; dithiocarbamate; Hirshfeld surface analysis.

CCDC reference: 1533246

Supporting information: this article has supporting information at journals.iucr.org/e

The title compound, $[Cd_2(C_8H_8NS_2)_4]$, is a centrosymmetric dimer with both chelating and μ_2-tridentate dithiocarbamate ligands. The resulting S_5 donor set defines a Cd^{II} coordination geometry intermediate between square-pyramidal and trigonal–bipyramidal, but tending towards the former. The packing features C—H···S and C—H···π interactions, which generate a three-dimensional network. The influence of these interactions, along with intra-dimer π–π interactions between chelate rings, has been investigated by an analysis of the Hirshfeld surface.

1. Chemical context

The structural chemistry of the binary zinc-triad (group 12) dithiocarbamates $(^-S_2CNRR')_2$ (R/R' = alkyl/aryl), along with related 1,1-dithiolate ligands, *i.e.* dithiophosphates $[^-S_2P(OR)_2]$ and dithiocarbonates (xanthates; ^-S_2COR), have long attracted the attention of structural chemists owing to their diversity of structures/supramolecular association patterns in the solid state (Cox & Tiekink, 1997; Tiekink, 2003). The common structural motif adopted by all elements is one that features two chelating ligands and two tridentate ligands (chelating one metal atom and simultaneously bridging to a second), leading, usually, to a centrosymmetric binuclear molecule. Indeed, most zinc dithiocarbamate structures adopt this motif, but when the R/R' are bulky, a mononuclear species with tetrahedrally coordinated zinc atoms is found; significantly greater structural variety has been noted for the binary zinc dithiophosphates and xanthates (Lai *et al.*, 2002; Tan *et al.*, 2015). More diversity in structural motifs is noted in the binary cadmium dithiocarbamates with the recent observation of linear polymeric forms with hexacoordinated cadmium atoms (Tan *et al.*, 2013, 2016; Ferreira *et al.*, 2016). Systematic studies indicated solvent-mediated transformations between polymeric and binuclear structural motifs, with the latter being the thermodynamically more stable (Tan *et al.*, 2013, 2016). The greatest structural diversity among the zinc-triad dithiocarbamates is found for the binary mercury compounds, where mononuclear, binuclear and polymeric structures have been observed, as summarized very recently (Jotani *et al.*, 2016). Complementing the structural motifs already mentioned for zinc and cadmium is a trinuclear species, {Hg[S_2CN(tetra-

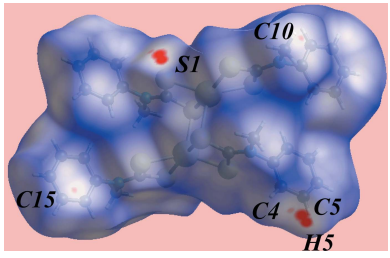

Table 1
Selected geometric parameters (Å, °).

Cd—S1	2.5044 (8)	C1—S2	1.739 (3)
Cd—S2	2.9331 (8)	C9—S3	1.730 (3)
Cd—S2^{i}	2.5942 (8)	C9—S4	1.717 (4)
Cd—S3	2.5397 (9)	C1—N1	1.326 (4)
Cd—S4	2.6196 (8)	C9—N2	1.344 (4)
C1—S1	1.716 (3)		
S1—Cd—S2	66.15 (2)	S2—Cd—S4	161.85 (3)
S1—Cd—S3	138.16 (3)	S2—Cd—S2^{i}	92.58 (2)
S1—Cd—S4	114.48 (3)	S3—Cd—S4	70.93 (3)
S1—Cd—S2^{i}	104.42 (3)	S3—Cd—S2^{i}	114.47 (3)
S2—Cd—S3	96.36 (2)	S4—Cd—S2^{i}	104.38 (3)

Symmetry code: (i) $-x, -y+1, -z+1$.

hydroquinoline)]$_2$}$_3$ (Rajput *et al.*, 2014), with the central Hg^{II} atom being hexacoordinated, as in the polymeric form, and the peripheral Hg^{II} atoms being coordinated as in the binuclear form, indicating the possibility that this is an intermediate metastable form in the crystallization of this compound. In light of the above, when crystals of the title compound became available, namely {Cd[S$_2$CN(Me)Ph]$_2$}$_2$, (I), its crystal and molecular structures were studied, along with an evaluation of the supramolecular association in the crystal through an analysis of the Hirshfeld surface.

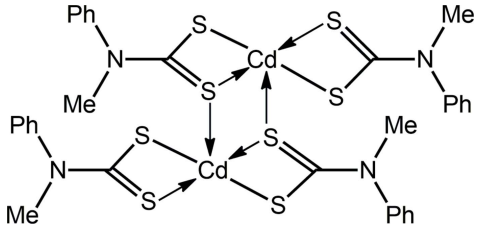

2. Structural commentary

The centrosymmetric binuclear molecule of (I) (Fig. 1) conforms to the common binuclear motif adopted by binary zinc-triad dithiocarbamates. The S1 dithiocarbamate anion forms a nearly symmetric bridge, as seen in the value of

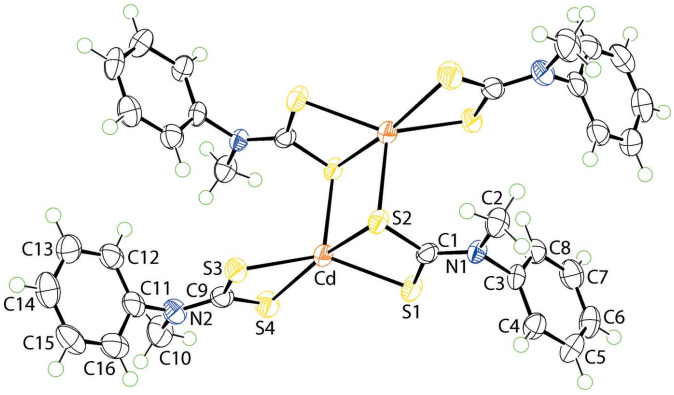

Figure 1
The molecular structure of (I), showing the atom-labelling scheme and displacement ellipsoids at the 70% probability level. The molecule is located about a centre of inversion and unlabelled atoms are generated by the symmetry operation $(-x, 1-y, 1-z)$.

Table 2
Hydrogen-bond geometry (Å, °).

*Cg*1 is the centroid of the C3–C8 ring.

D—H···*A*	*D*—H	H···*A*	*D*···*A*	*D*—H···*A*
C14—H14···*Cg*1^{ii}	0.95	2.99	3.883 (4)	156
C5—H5···S1^{iii}	0.95	2.75	3.372 (4)	124

Symmetry codes: (ii) $x+1, -y+\frac{1}{2}, z-\frac{1}{2}$; (iii) $-x, y+\frac{1}{2}, -z+\frac{1}{2}$.

Δ(Cd—S) = 0.09 Å = Cd—S$_{long}$ − Cd—S$_{short}$. Within the resultant {CdSCS}$_2$ eight-membered ring, which adopts a chair conformation, the bridging S2 atom also forms a longer [S2—Cd^{i} = 2.9331 (8) Å; symmetry code: (i) $-x, 1-y, 1-z$] transannular interaction. The S3 dithiocarbamate ligand is strictly chelating, with Δ(Cd—S) = 0.08 Å. Reflecting the symmetric modes of coordination of the dithiocarbamate ligands, the C—S bond lengths are equal within 5σ (Table 1).

The resultant S$_5$ donor set defines a highly distorted pentacoordinate geometry, with the major distortions due to the disparate Cd—S bond lengths and the acute angles subtended at the Cd^{II} atom by the chelating ligands (Table 1). The widest angle at the Cd^{II} atom involves the S atoms forming the weaker Cd—S interactions, *i.e.* S2—Cd—S4 = 161.85 (3)°. A measure of the distortion of a coordination

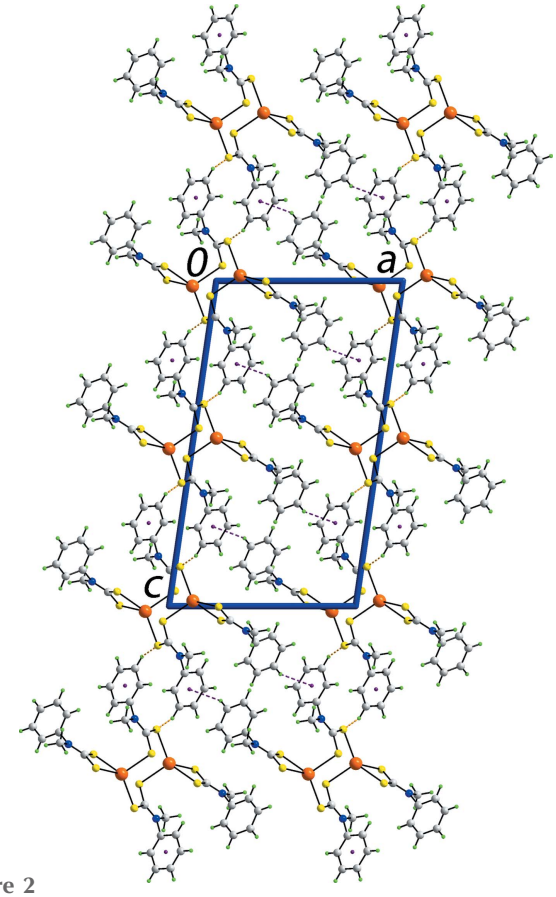

Figure 2
A view of the unit-cell contents of (I) in projection down the *b* axis. The C—H···π(chelate ring) and C—H···S interactions are shown as purple and orange dashed lines, respectively.

Table 3
Short interatomic contacts (Å) in (I).

Contact	Distance	Symmetry operation
S1···C4	3.462 (3)	$-x, -\frac{1}{2}+y, -z$
S1···H4	2.94	$-x, -\frac{1}{2}+y, -z$
S3···H16	2.88	$1-x, 1-y, 1-z$
C10···C15	3.376 (5)	$x, -1+y, z$
C7···H2*B*	2.89	$x, -1+y, z$
C13···H7	2.84	$1-x, -y, z$
C14···H7	2.87	$1-x, -y, z$
C14···H10*C*	2.81	$x, 1+y, z$
C15···H6	2.84	$1-x, -y, z$

geometry from the ideal square-pyramidal and trigonal–bipyramidal geometries is given by the value of τ (Addison *et al.*, 1984), which computes to 0.0 and 1.0 for the ideal geometries, respectively. In (I), the value of τ is 0.39, *i.e.* intermediate between the two extremes, but tending towards the former.

3. Supramolecular features

Two specific intermolecular interactions have been identified in the molecular packing of (I), and each involves the participation of phenyl ring C3–C8 (Table 2). Phenyl-C—H···π interactions with the C3–C8 ring as the acceptor lead to supramolecular layers parallel to ($\bar{1}$02), as each binuclear molecule participates in four such interactions. The layers are connected into a three-dimensional architecture by phenyl-C—H···S interactions, *i.e.* with the C3–C8 ring as donor (Fig. 2).

4. Hirshfeld surface analysis

The Hirshfeld surface analysis for (I) was performed as described in a recent report of a related binuclear cadmium dithiocarbamate compound (Jotani *et al.*, 2016). On the Hirshfeld surface mapped over d_{norm} in the range −0.055 to 1.371 au (Fig. 3), the bright-red spots near the C5, H5 and S1 atoms indicate respective donors and acceptors of intermolecular C—H···S interactions; the other pair of faint-red spots near atoms C4 and S1 represent a weaker interaction

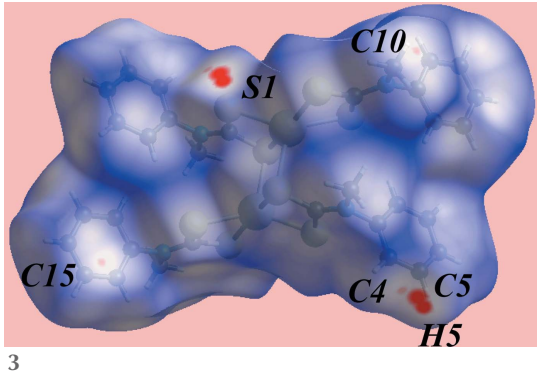

Figure 3
A view of the Hirshfeld surface for (I) mapped over d_{norm} in the range −0.055 to 1.371 au.

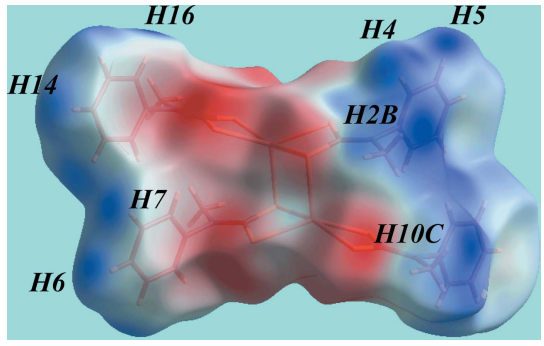

Figure 4
A view of Hirshfeld surface for (I) mapped over the electrostatic potential in the range ±0.048 au.

(Table 3). The donors and acceptors of the specified C—H···S and C—H···π interactions in Table 2, and short interatomic C···H/H···C contacts (Table 3) give rise to positive and negative potentials, respectively, and are viewed as the blue

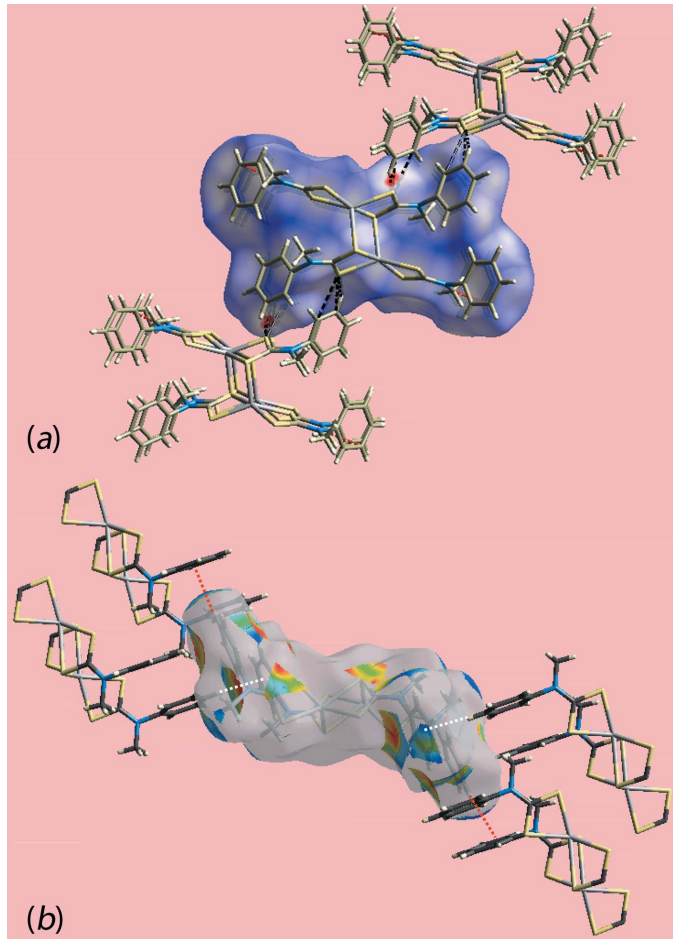

Figure 5
Views of the Hirshfeld surface mapped over (*a*) d_{norm} about a reference molecule, highlighting the intermolecular C—H···S interactions and short interatomic C···C contacts as black and red dashed lines, respectively, and (*b*) with shape-index property about a reference molecule. The C—H···π and π···H—C interactions are indicated with red and white dotted lines, respectively.

Table 4
Percentage contributions of the different intermolecular contacts to the Hirshfeld surface in (I).

Contact	% Contribution in (I)
H···H	40.0
S···H/H···S	26.7
C···H/H···C	24.8
S···S	5.8
Cd···H/H···Cd	1.2
N···H/H···N	0.8
Cd···S/S···Cd	0.7

and red regions on Hirshfeld surface mapped over electrostatic potential (in the range ±0.048 au) (Fig. 4). The immediate environments about a reference molecule within d_{norm} and shape-index mapped Hirshfeld surface are illustrated in Figs. 5(*a*) and 5(*b*), respectively, and again highlight the influence of C—H···S interactions, short C10···C15 contacts and C—H···π interactions involving phenyl rings (atoms C3–C8) as the acceptor. Thus, the C—H···S interactions involving the phenyl-ring C4, C5 and H5 atoms with S1 are shown with black dashed lines in Fig. 5(*a*); the red dashed lines indicate short interatomic C···C contacts (Table 3). The C—H···π and their reciprocal contacts, *i.e.* π···H—C, with phenyl-ring atom C14 as donor and phenyl ring C3–C8 as acceptor, are shown with red and white dotted lines, respectively, on the Hirshfeld surface mapped with shape-index property in Fig. 5(*b*).

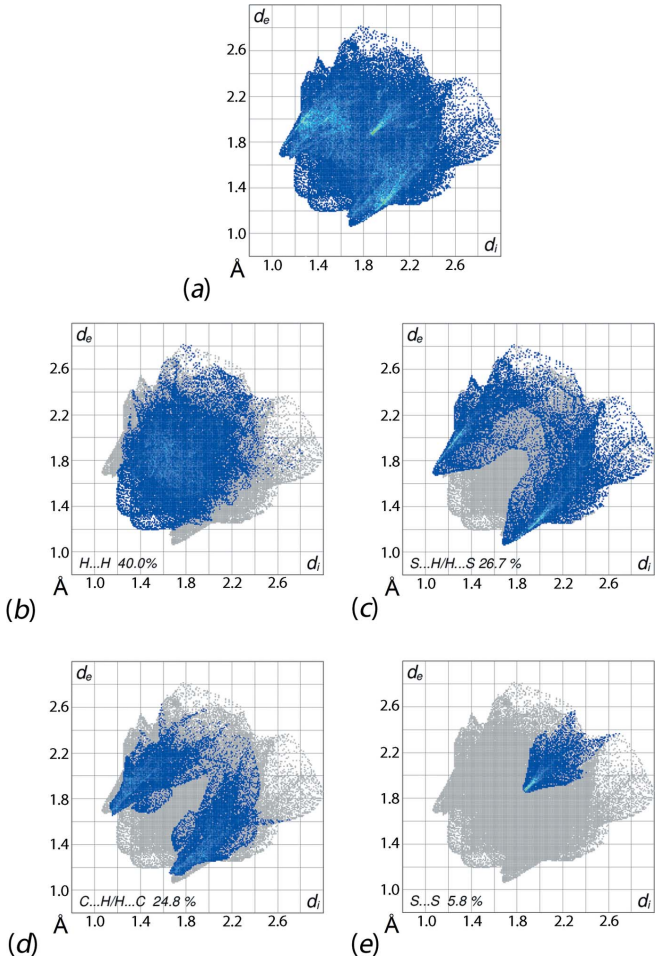

Figure 6
Fingerprint plots for (I): (*a*) overall and those delineated into (*b*) H···H, (*c*) S···H/H···S, (*d*) C···H/H···C and (*e*) S···S contacts.

The overall two-dimensional fingerprint plot and those delineated into H···H, S···H/H···S, C···H/H···C and S···S contacts (McKinnon *et al.*, 2007) are illustrated in Figs. 6(*a*)–(*e*); their relative contributions to the Hirshfeld surface are summarized quantitatively in Table 4. The relatively low contribution of H···H contacts to the Hirshfeld surface results from the involvement of surface H atoms in intermolecular C—H···S, C—H···π and C···H/H···C contacts. It is apparent from the fingerprint plot delineated into H···H contacts (Fig. 6*b*) that H···H contacts do not exert much influence on the molecular packing, as their interatomic distances are greater than the sum of their van der Waals radii, *i.e.* $d_e + d_i >$ 2.8 Å. A pair of peaks appearing in the fingerprint plot delineated into S···H/H···S contacts at $d_e + d_i \sim 2.8$ Å (Fig. 6*c*) arise from the C5—H5···S1 interaction; the weaker C4···H4···S1 interaction and short interatomic H···S/S···H contacts involving the S3 atom (Table 3) are viewed as a pair of thin green lines aligned at $d_e + d_i \sim 2.9$ Å.

The distribution of points showing the superimposition of a forceps-like shape on characteristic wings in the fingerprint plot delineated into C···H/H···C contacts (Fig. 6*d*) indicate the significance of these contacts through the presence of C—H···π interactions and short interatomic C···H/H···C contacts in the crystal. A pair of green lines within the forceps also indicates the influence of these contacts. Finally, an arrow-shaped distribution of green points in the centre in the plot corresponding to S···S contacts (Fig. 6*e*), together with the contribution from Cd···S/S···Cd contacts to the Hirshfeld surface (Table 4), show the presence of intramolecular π–π stacking interactions between the Cd/S1/C1/S2 chelate rings of inversion-related molecules [Cg···Cg = 3.6117 (11) Å; symmetry code: $-x$, $1-y$, $1-z$]. The small contributions from Cd···H/H···Cd and N···H/H···N contacts (Table 4) do not impact significantly on the molecular packing.

5. Database survey

The dithiocarbamate ligand featured in (I) has been reported in several other crystal structures (Groom *et al.*, 2016). Indeed, the binary zinc (Baba *et al.*, 2002) and mercury (Onwudiwe & Ajibade, 2011*a*,*b*) structures have been reported already, so, in this sense, the structure of (I) completes the series. The zinc compound adopts the common binuclear motif (Baba *et al.*, 2002). More interesting is the fact that for the mercury structure, both mononuclear (Onwudiwe & Ajibade, 2011*a*) and binuclear (Onwudiwe & Ajibade, 2011*b*) forms have been reported (Tan *et al.*, 2015). As to the other main group element structures, the binary dithiocarbamate compounds of antimony(III) (Baba *et al.*, 2003) and bismuth(III) (Yin *et al.*, 2004), including an acetonitrile solvate (Lai & Tiekink, 2007), have been described. These, too, present the same structural features as reported for the overwhelming majority of related

antimony(III) (Liu & Tiekink, 2005) and bismuth(III) dithiocarbamate compounds (Lai & Tiekink, 2007).

6. Synthesis and crystallization

All chemicals and solvents were used as purchased without purification, and all reactions were carried out under ambient conditions. The melting point was determined using an Electrothermal digital melting-point apparatus and was uncorrected. The IR spectrum was obtained on a PerkinElmer Spectrum 400 FT Mid-IR/Far-IR spectrophotometer from 4000 to 400 cm^{-1}. ^1H and ^{13}C NMR spectra were recorded at room temperature in DMSO-d_6 solution on a Jeol ECA 400 MHz FT–NMR spectrometer.

Sodium methylphenyldithiocarbamate (1.0 mmol, 0.205 g) in methanol (25 ml) was added to cadmium chloride (1.0 mmol, 0.183 g) in methanol (10 ml). The resulting mixture was stirred and refluxed for 2 h. The filtrate was evaporated until an off-white precipitate was obtained, which was recrystallized in methanol. Slow evaporation of the filtrate yielded colourless crystals of the title compound (yield: 0.194 g, 61%; m.p. 473 K). IR (cm^{-1}): 1491 (*m*) [ν(C—N)], 1160 (*m*), 964 (*s*) [ν(C—S)] cm^{-1}. ^1H NMR: δ 7.26–7.42 (*m*, 5H, aromatic H), 2.05 (*s*, 3H, CH_3). ^{13}C NMR: δ 46.6 (Me) 125.6, 128.4, 129.6, 147.9 (aromatic C), 207.8 (CS_2).

7. Refinement

Crystal data, data collection and structure refinement details are summarized in Table 5. Carbon-bound H atoms were placed in calculated positions (C—H = 0.95–0.98 Å) and were included in the refinement in the riding-model approximation, with U_{iso}(H) values set at 1.2–1.5U_{eq}(C).

Table 5
Experimental details.

Crystal data	
Chemical formula	$[Cd_2(C_8H_8NS_2)_4]$
M_r	953.92
Crystal system, space group	Monoclinic, $P2_1/c$
Temperature (K)	100
a, b, c (Å)	12.7972 (6), 6.4445 (3), 22.582 (1)
β (°)	98.247 (4)
V (Å^3)	1843.11 (15)
Z	2
Radiation type	Mo $K\alpha$
μ (mm^{-1})	1.64
Crystal size (mm)	0.20 × 0.15 × 0.10
Data collection	
Diffractometer	Agilent SuperNova Dual Source diffractometer with an Atlas detector
Absorption correction	Multi-scan (*CrysAlis PRO*; Agilent, 2013)
T_{min}, T_{max}	0.731, 1.000
No. of measured, independent and observed [$I > 2\sigma(I)$] reflections	11881, 4894, 3804
R_{int}	0.037
(sin $\theta/\lambda)_{max}$ (Å^{-1})	0.708
Refinement	
$R[F^2 > 2\sigma(F^2)]$, $wR(F^2)$, S	0.037, 0.086, 1.05
No. of reflections	4894
No. of parameters	210
H-atom treatment	H-atom parameters constrained
$\Delta\rho_{max}$, $\Delta\rho_{min}$ (e Å^{-3})	0.72, −0.48

Computer programs: *CrysAlis PRO* (Agilent, 2013), *SHELXS97* (Sheldrick, 2008), *SHELXL2014* (Sheldrick, 2015), *ORTEP-3 for Windows* (Farrugia, 2012), *DIAMOND* (Brandenburg, 2006) and *publCIF* (Westrip, 2010).

Acknowledgements

The authors are grateful to Sunway University and the Ministry of Higher Education of Malaysia (MOHE) Fundamental Research Grant Scheme for supporting this research.

Funding information

Funding for this research was provided by: Ministry of Higher Education of Malaysia (MOHE) (award No. FP033-2014B).

References

Addison, A. W., Rao, T. N., Reedijk, J., van Rijn, J. & Verschoor, G. C. (1984). *J. Chem. Soc. Dalton Trans.* pp. 1349–1356.
Agilent (2013). *CrysAlis PRO*. Agilent Technologies Inc., Santa Clara, CA, USA.
Baba, I., Lee, L. H., Farina, Y., Othman, A. H., Ibrahim, A. R., Usman, A., Fun, H.-K. & Ng, S. W. (2002). *Acta Cryst.* E**58**, m744–m745.
Baba, I., Skelton, B. W. & White, A. H. (2003). *Aust. J. Chem.* **56**, 27–29.
Brandenburg, K. (2006). *DIAMOND*. Crystal Impact GbR, Bonn, Germany.
Cox, M. J. & Tiekink, E. R. T. (1997). *Rev. Inorg. Chem.* **17**, 1–23.
Farrugia, L. J. (2012). *J. Appl. Cryst.* **45**, 849–854.
Ferreira, I. P., de Lima, G. M., Paniago, E. B., Pinheiro, C. B., Wardell, J. L. & Wardell, S. M. S. V. (2016). *Inorg. Chim. Acta*, **441**, 137–145.
Groom, C. R., Bruno, I. J., Lightfoot, M. P. & Ward, S. C. (2016). *Acta Cryst.* B**72**, 171–179.
Jotani, M. M., Poplaukhin, P., Arman, H. D. & Tiekink, E. R. T. (2016). *Acta Cryst.* E**72**, 1085–1092.
Lai, C. S., Lim, Y. X., Yap, T. C. & Tiekink, E. R. T. (2002). *CrystEngComm*, **4**, 596–600.
Lai, C. S. & Tiekink, E. R. T. (2007). *Z. Kristallogr.* **222**, 532–538.
Liu, Y. & Tiekink, E. R. T. (2005). *CrystEngComm*, **7**, 20–27.
McKinnon, J. J., Jayatilaka, D. & Spackman, M. A. (2007). *Chem. Commun.* pp. 3814–3816.
Onwudiwe, D. C. & Ajibade, P. A. (2011*a*). *J. Coord. Chem.* **64**, 2963–2973.
Onwudiwe, D. C. & Ajibade, P. A. (2011*b*). *Int. J. Mol. Sci.* **12**, 1964–1978.
Rajput, G., Yadav, M. K., Thakur, T. S., Drew, M. G. B. & Singh, N. (2014). *Polyhedron*, **69**, 225–233.
Sheldrick, G. M. (2008). *Acta Cryst.* A**64**, 112–122.
Sheldrick, G. M. (2015). *Acta Cryst.* C**71**, 3–8.
Tan, Y. S., Halim, S. N. A. & Tiekink, E. R. T. (2016). *Z. Kristallogr.* **231**, 113–126.
Tan, Y. S., Ooi, K. K., Ang, K. P., Akim, A. M., Cheah, Y.-K., Halim, S. N. A., Seng, H.-L. & Tiekink, E. R. T. (2015). *J. Inorg. Biochem.* **150**, 48–62.
Tan, Y. S., Sudlow, A. L., Molloy, K. C., Morishima, Y., Fujisawa, K., Jackson, W. J., Henderson, W., Halim, S. N., Bt, A., Ng, S. W. & Tiekink, E. R. T. (2013). *Cryst. Growth Des.* **13**, 3046–3056.
Tiekink, E. R. T. (2003). *CrystEngComm*, **5**, 101–113.
Westrip, S. P. (2010). *J. Appl. Cryst.* **43**, 920–925.
Yin, H.-D., Wang, C.-H. & Wang, Y. (2004). *Appl. Organomet. Chem.* **18**, 199–200.

supporting information

Acta Cryst. (2017). E**73**, 429-433 [https://doi.org/10.1107/S2056989017002705]

Bis(μ_2-*N*-methyl-*N*-phenyldithiocarbamato)-$\kappa^3 S,S':S;\kappa^3 S:S,S'$-bis[(*N*-methyl-*N*-phenyldithiocarbamato-$\kappa^2 S,S'$)cadmium]: crystal structure and Hirshfeld surface analysis

Siti Aisyah Nabilah Suwardi, See Mun Lee, Kong Mun Lo, Mukesh M. Jotani and Edward R. T. Tiekink

Computing details

Data collection: *CrysAlis PRO* (Agilent, 2013); cell refinement: *CrysAlis PRO* (Agilent, 2013); data reduction: *CrysAlis PRO* (Agilent, 2013); program(s) used to solve structure: *SHELXS97* (Sheldrick, 2008); program(s) used to refine structure: *SHELXL2014* (Sheldrick, 2015); molecular graphics: *ORTEP-3 for Windows* (Farrugia, 2012) and *DIAMOND* (Brandenburg, 2006); software used to prepare material for publication: *publCIF* (Westrip, 2010).

Bis(μ_2-*N*-methyl-*N*-phenyldithiocarbamato)-$\kappa^3 S,S':S;\kappa^3 S:S,S'$-bis[(*N*-methyl-*N*-phenyldithiocarbamato-$\kappa^2 S,S'$)cadmium(II)]

Crystal data

$[Cd_2(C_8H_8NS_2)_4]$
M_r = 953.92
Monoclinic, $P2_1/c$
a = 12.7972 (6) Å
b = 6.4445 (3) Å
c = 22.582 (1) Å
β = 98.247 (4)°
V = 1843.11 (15) Å^3
Z = 2
$F(000)$ = 952
D_x = 1.719 Mg m^{-3}
Mo $K\alpha$ radiation, λ = 0.71073 Å
Cell parameters from 4387 reflections
θ = 3.4–29.8°
μ = 1.64 mm^{-1}
T = 100 K
Block, colourless
0.20 × 0.15 × 0.10 mm

Data collection

Agilent SuperNova Dual Source diffractometer with an Atlas detector
Radiation source: SuperNova (Mo) X-ray Source
Mirror monochromator
Detector resolution: 10.4041 pixels mm^{-1}
ω scan
Absorption correction: multi-scan (CrysAlis PRO; Agilent, 2013)
T_{min} = 0.731, T_{max} = 1.000
11881 measured reflections
4894 independent reflections
3804 reflections with $I > 2\sigma(I)$
R_{int} = 0.037
θ_{max} = 30.2°, θ_{min} = 3.2°
h = −12→17
k = −9→8
l = −29→30

Refinement

Refinement on F^2
Least-squares matrix: full
$R[F^2 > 2\sigma(F^2)] = 0.037$
$wR(F^2) = 0.086$
$S = 1.05$
4894 reflections
210 parameters
0 restraints

Primary atom site location: structure-invariant direct methods
Hydrogen site location: inferred from neighbouring sites
H-atom parameters constrained
$w = 1/[\sigma^2(F_o^2) + (0.0331P)^2 + 0.5876P]$ where $P = (F_o^2 + 2F_c^2)/3$
$(\Delta/\sigma)_{max} = 0.001$
$\Delta\rho_{max} = 0.72$ e Å^{-3}
$\Delta\rho_{min} = -0.48$ e Å^{-3}

Special details

Geometry. All esds (except the esd in the dihedral angle between two l.s. planes) are estimated using the full covariance matrix. The cell esds are taken into account individually in the estimation of esds in distances, angles and torsion angles; correlations between esds in cell parameters are only used when they are defined by crystal symmetry. An approximate (isotropic) treatment of cell esds is used for estimating esds involving l.s. planes.

Fractional atomic coordinates and isotropic or equivalent isotropic displacement parameters (Å²)

	x	*y*	*z*	U_{iso}*/U_{eq}
Cd	0.12343 (2)	0.35538 (4)	0.48383 (2)	0.02641 (8)
S1	0.02923 (7)	0.37408 (12)	0.37881 (4)	0.02834 (19)
S2	0.02121 (6)	0.75614 (12)	0.45307 (3)	0.02341 (17)
S3	0.28949 (6)	0.50187 (12)	0.54452 (4)	0.02566 (18)
S4	0.26597 (7)	0.06179 (13)	0.50220 (4)	0.0311 (2)
N1	−0.09657 (19)	0.6884 (4)	0.34672 (11)	0.0205 (5)
N2	0.4316 (2)	0.2090 (4)	0.57566 (12)	0.0287 (6)
C1	−0.0239 (2)	0.6135 (5)	0.38915 (13)	0.0220 (6)
C2	−0.1463 (3)	0.8929 (5)	0.34931 (15)	0.0286 (7)
H2A	−0.2198	0.8754	0.3559	0.043*
H2B	−0.1443	0.9663	0.3115	0.043*
H2C	−0.1078	0.9736	0.3823	0.043*
C3	−0.1353 (2)	0.5650 (5)	0.29431 (13)	0.0217 (6)
C4	−0.0939 (3)	0.5954 (5)	0.24187 (14)	0.0271 (7)
H4	−0.0392	0.6940	0.2401	0.033*
C5	−0.1334 (3)	0.4800 (5)	0.19168 (15)	0.0314 (8)
H5	−0.1055	0.4999	0.1553	0.038*
C6	−0.2119 (3)	0.3383 (5)	0.19425 (16)	0.0334 (8)
H6	−0.2381	0.2593	0.1598	0.040*
C7	−0.2535 (3)	0.3093 (5)	0.24708 (17)	0.0334 (8)
H7	−0.3084	0.2111	0.2487	0.040*
C8	−0.2150 (2)	0.4235 (5)	0.29753 (15)	0.0271 (7)
H8	−0.2432	0.4045	0.3338	0.032*
C9	0.3372 (2)	0.2509 (5)	0.54363 (14)	0.0257 (7)
C10	0.4776 (3)	0.0001 (5)	0.57988 (17)	0.0398 (9)
H10A	0.5511	0.0070	0.5724	0.060*
H10B	0.4372	−0.0902	0.5500	0.060*
H10C	0.4752	−0.0560	0.6200	0.060*
C11	0.4909 (2)	0.3640 (5)	0.61192 (15)	0.0278 (7)

C12	0.4636 (3)	0.4133 (5)	0.66742 (15)	0.0303 (7)
H12	0.4045	0.3484	0.6808	0.036*
C13	0.5227 (3)	0.5572 (6)	0.70328 (16)	0.0345 (8)
H13	0.5038	0.5920	0.7412	0.041*
C14	0.6088 (3)	0.6503 (5)	0.68420 (17)	0.0378 (9)
H14	0.6491	0.7494	0.7089	0.045*
C15	0.6364 (3)	0.5989 (6)	0.62904 (18)	0.0367 (9)
H15	0.6965	0.6615	0.6162	0.044*
C16	0.5770 (3)	0.4566 (5)	0.59235 (16)	0.0329 (8)
H16	0.5953	0.4232	0.5542	0.039*

Atomic displacement parameters (Å²)

	U^{11}	U^{22}	U^{33}	U^{12}	U^{13}	U^{23}
Cd	0.02523 (14)	0.03538 (16)	0.01777 (12)	0.00772 (10)	0.00019 (9)	0.00105 (10)
S1	0.0369 (5)	0.0274 (4)	0.0186 (4)	0.0104 (4)	−0.0034 (3)	−0.0032 (3)
S2	0.0267 (4)	0.0251 (4)	0.0172 (4)	0.0002 (3)	−0.0014 (3)	−0.0024 (3)
S3	0.0252 (4)	0.0258 (4)	0.0251 (4)	0.0074 (3)	0.0005 (3)	0.0023 (3)
S4	0.0325 (5)	0.0277 (4)	0.0319 (5)	0.0082 (4)	0.0001 (3)	−0.0026 (4)
N1	0.0237 (13)	0.0209 (13)	0.0161 (12)	0.0013 (10)	−0.0002 (10)	0.0015 (10)
N2	0.0266 (14)	0.0273 (14)	0.0315 (16)	0.0099 (12)	0.0017 (12)	0.0024 (12)
C1	0.0239 (16)	0.0259 (17)	0.0168 (15)	−0.0029 (13)	0.0051 (12)	0.0014 (12)
C2	0.0355 (19)	0.0213 (16)	0.0271 (18)	0.0041 (14)	−0.0019 (14)	0.0021 (13)
C3	0.0238 (15)	0.0208 (15)	0.0184 (15)	0.0022 (13)	−0.0039 (11)	0.0015 (12)
C4	0.0293 (17)	0.0289 (17)	0.0221 (16)	−0.0056 (14)	0.0000 (13)	0.0004 (13)
C5	0.042 (2)	0.0311 (18)	0.0196 (16)	−0.0015 (16)	−0.0005 (14)	0.0018 (14)
C6	0.0358 (19)	0.0315 (19)	0.0285 (19)	−0.0031 (15)	−0.0106 (14)	−0.0058 (15)
C7	0.0269 (18)	0.0319 (18)	0.039 (2)	−0.0059 (15)	−0.0027 (14)	−0.0007 (16)
C8	0.0249 (16)	0.0290 (17)	0.0267 (17)	0.0022 (14)	0.0017 (13)	0.0026 (14)
C9	0.0256 (17)	0.0294 (18)	0.0230 (16)	0.0072 (14)	0.0059 (12)	0.0042 (14)
C10	0.041 (2)	0.033 (2)	0.042 (2)	0.0175 (16)	−0.0041 (16)	0.0032 (17)
C11	0.0216 (16)	0.0307 (18)	0.0301 (18)	0.0101 (14)	0.0002 (13)	0.0079 (14)
C12	0.0242 (17)	0.0356 (19)	0.0309 (19)	0.0053 (15)	0.0030 (14)	0.0096 (15)
C13	0.0335 (19)	0.039 (2)	0.0290 (19)	0.0069 (16)	−0.0007 (15)	0.0040 (16)
C14	0.033 (2)	0.033 (2)	0.043 (2)	0.0031 (16)	−0.0094 (16)	0.0071 (17)
C15	0.0211 (17)	0.038 (2)	0.051 (2)	0.0048 (15)	0.0048 (15)	0.0161 (17)
C16	0.0290 (18)	0.0348 (19)	0.036 (2)	0.0103 (16)	0.0079 (15)	0.0112 (16)

Geometric parameters (Å, º)

Cd—S1	2.5044 (8)	C4—H4	0.9500
Cd—S2	2.9331 (8)	C5—C6	1.365 (5)
Cd—S2^{i}	2.5942 (8)	C5—H5	0.9500
Cd—S3	2.5397 (9)	C6—C7	1.387 (5)
Cd—S4	2.6196 (8)	C6—H6	0.9500
C1—S1	1.716 (3)	C7—C8	1.386 (5)
C1—S2	1.739 (3)	C7—H7	0.9500
S2—Cd^{i}	2.5942 (8)	C8—H8	0.9500

C9—S3	1.730 (3)	C10—H10A	0.9800
C9—S4	1.717 (4)	C10—H10B	0.9800
C1—N1	1.326 (4)	C10—H10C	0.9800
N1—C3	1.453 (4)	C11—C16	1.380 (5)
N1—C2	1.468 (4)	C11—C12	1.386 (5)
C9—N2	1.344 (4)	C12—C13	1.383 (5)
N2—C11	1.438 (4)	C12—H12	0.9500
N2—C10	1.467 (4)	C13—C14	1.377 (5)
C2—H2A	0.9800	C13—H13	0.9500
C2—H2B	0.9800	C14—C15	1.383 (5)
C2—H2C	0.9800	C14—H14	0.9500
C3—C8	1.378 (4)	C15—C16	1.387 (5)
C3—C4	1.379 (4)	C15—H15	0.9500
C4—C5	1.389 (4)	C16—H16	0.9500

S1—Cd—S2	66.15 (2)	C6—C5—H5	119.8
S1—Cd—S3	138.16 (3)	C4—C5—H5	119.8
S1—Cd—S4	114.48 (3)	C5—C6—C7	120.1 (3)
S1—Cd—S2^{i}	104.42 (3)	C5—C6—H6	119.9
S2—Cd—S3	96.36 (2)	C7—C6—H6	119.9
S2—Cd—S4	161.85 (3)	C8—C7—C6	120.0 (3)
S2—Cd—S2^{i}	92.58 (2)	C8—C7—H7	120.0
S3—Cd—S4	70.93 (3)	C6—C7—H7	120.0
S3—Cd—S2^{i}	114.47 (3)	C3—C8—C7	119.1 (3)
S4—Cd—S2^{i}	104.38 (3)	C3—C8—H8	120.5
C1—S1—Cd	93.49 (11)	C7—C8—H8	120.5
C1—S2—Cd^{i}	97.54 (10)	N2—C9—S4	121.1 (2)
C1—S2—Cd	79.34 (11)	N2—C9—S3	118.3 (3)
Cd^{i}—S2—Cd	87.43 (2)	S4—C9—S3	120.62 (19)
C9—S3—Cd	85.16 (11)	N2—C10—H10A	109.5
C9—S4—Cd	82.93 (11)	N2—C10—H10B	109.5
C1—N1—C3	120.7 (3)	H10A—C10—H10B	109.5
C1—N1—C2	124.1 (3)	N2—C10—H10C	109.5
C3—N1—C2	115.2 (2)	H10A—C10—H10C	109.5
C9—N2—C11	121.8 (3)	H10B—C10—H10C	109.5
C9—N2—C10	122.8 (3)	C16—C11—C12	120.5 (3)
C11—N2—C10	115.3 (3)	C16—C11—N2	119.9 (3)
N1—C1—S1	118.6 (2)	C12—C11—N2	119.6 (3)
N1—C1—S2	121.5 (2)	C13—C12—C11	119.7 (3)
S1—C1—S2	119.82 (18)	C13—C12—H12	120.1
N1—C2—H2A	109.5	C11—C12—H12	120.1
N1—C2—H2B	109.5	C14—C13—C12	120.3 (3)
H2A—C2—H2B	109.5	C14—C13—H13	119.9
N1—C2—H2C	109.5	C12—C13—H13	119.9
H2A—C2—H2C	109.5	C13—C14—C15	119.8 (4)
H2B—C2—H2C	109.5	C13—C14—H14	120.1
C8—C3—C4	121.2 (3)	C15—C14—H14	120.1
C8—C3—N1	119.2 (3)	C14—C15—C16	120.5 (3)

C4—C3—N1	119.6 (3)	C14—C15—H15	119.8
C3—C4—C5	119.0 (3)	C16—C15—H15	119.8
C3—C4—H4	120.5	C11—C16—C15	119.3 (3)
C5—C4—H4	120.5	C11—C16—H16	120.4
C6—C5—C4	120.5 (3)	C15—C16—H16	120.4
C3—N1—C1—S1	3.9 (4)	C6—C7—C8—C3	−0.1 (5)
C2—N1—C1—S1	−178.4 (2)	C11—N2—C9—S4	−178.2 (2)
C3—N1—C1—S2	−178.5 (2)	C10—N2—C9—S4	−3.1 (4)
C2—N1—C1—S2	−0.7 (4)	C11—N2—C9—S3	2.5 (4)
Cd—S1—C1—N1	−170.8 (2)	C10—N2—C9—S3	177.6 (2)
Cd—S1—C1—S2	11.52 (17)	Cd—S4—C9—N2	174.9 (3)
Cd^{i}—S2—C1—N1	86.5 (2)	Cd—S4—C9—S3	−5.81 (16)
Cd—S2—C1—N1	172.4 (2)	Cd—S3—C9—N2	−174.7 (3)
Cd^{i}—S2—C1—S1	−95.91 (17)	Cd—S3—C9—S4	5.96 (17)
Cd—S2—C1—S1	−9.98 (15)	C9—N2—C11—C16	−103.8 (4)
C1—N1—C3—C8	83.8 (4)	C10—N2—C11—C16	80.7 (4)
C2—N1—C3—C8	−94.1 (3)	C9—N2—C11—C12	78.8 (4)
C1—N1—C3—C4	−98.0 (3)	C10—N2—C11—C12	−96.7 (4)
C2—N1—C3—C4	84.1 (3)	C16—C11—C12—C13	0.4 (5)
C8—C3—C4—C5	−0.3 (5)	N2—C11—C12—C13	177.8 (3)
N1—C3—C4—C5	−178.4 (3)	C11—C12—C13—C14	−0.5 (5)
C3—C4—C5—C6	−0.1 (5)	C12—C13—C14—C15	−0.2 (5)
C4—C5—C6—C7	0.4 (5)	C13—C14—C15—C16	1.0 (5)
C5—C6—C7—C8	−0.4 (5)	C12—C11—C16—C15	0.4 (5)
C4—C3—C8—C7	0.4 (5)	N2—C11—C16—C15	−177.0 (3)
N1—C3—C8—C7	178.5 (3)	C14—C15—C16—C11	−1.1 (5)

Symmetry code: (i) −*x*, −*y*+1, −*z*+1.

Hydrogen-bond geometry (Å, º)

*Cg*1 is the ring centroid of the C3–C8 ring.

D—H···*A*	*D*—H	H···*A*	*D*···*A*	*D*—H···*A*
C14—H14···*Cg*1^{ii}	0.95	2.99	3.883 (4)	156
C5—H5···S1^{iii}	0.95	2.75	3.372 (4)	124

Symmetry codes: (ii) *x*+1, −*y*+1/2, *z*−1/2; (iii) −*x*, *y*+1/2, −*z*+1/2.